Articles

Thermal Phase Transition of Cesium Formate

Yoshio Masuda,* Akihiko Yahata, and Hiroshi Ogawa

Departments of Environmental Science and Chemistry, Faculty of Science, Niigata University, Niigata 950-21, Japan

Received October 12, 1994[⊗]

The phase transition of cesium formate observed at around 36 °C was found to be a reversible first-order transition by means of thermal analyses. The results of the Rietveld analysis of powder X-ray diffraction data showed that an orthorhombic phase (*Pbcm*, $Z = 8$; $a = 4.785(1)$, $b = 9.553(9)$, and $c = 15.927(2)$ Å) transformed to a cubic phase (*Pm3m*, $Z = 1$; $a = 4.500(5)$ Å). The large values of enthalpy and entropy change for the transition ($\Delta H_{tr} = 6.87 \pm 0.28$ kJ mol^{-1} and $\Delta S_{tr} = 22.2 \pm 0.9$ J K^{-1} mol^{-1}) were discussed on the basis of the change of the orientation freedom of the formate ion.

Introduction

Thermal behavior of alkali metal formates has been widely studied by means of thermal analyses such as thermogravimetry (TG), differential thermal analysis (DTA), and differential scanning calorimetry (DSC) by Masuda and Shishido.[1-3] When these compounds were heated, they melted at first and then decomposed through two stages. In the first stage, oxalates and carbonates were formed simultaneously. In the second stage, the oxalates formed in the first stage decomposed to carbonate and carbon monoxide. The authors described in detail these decomposition processes and the atmospheric effect on these decompositions. In an earlier thermal analysis of alkali metal formates it was found that the phases of anhydrous lithium, sodium, and potassium formates transformed immediately before melting.[4] Braghetti and Berchiesi found the existence of phase transitions for rubidium and cesium formates and reported the values of enthalpy and entropy changes for the phase transitions and melting of these metal formates.[5] However, these authors did not study the phase transitions from the viewpoint of the structural changes.

In the present paper, the crystal structures of cesium formate, both before and after the phase transition, were determined by means of the Rietveld method.[6] The enthalpy and entropy changes for the phase transition are discussed on the basis of the structural changes.

Experimental Section

Cesium formate was directly synthesized as follows: 100 mL of 0.5 mol dm^{-3} formic acid was added to an aqueous solution of 50 mL of 0.5 mol dm^{-3} cesium carbonate. The mixture was stirred for 5 h at 80 °C. After slow evaporation of this mixture, a residual crystalline material was obtained. The compound was recrystallized from distilled water and identified by means of IR and TG measurements. The compound was so hygroscopic that it was kept in a desiccator under vacuum, and it was dried in an oven above 100 °C for 1 week before measurement.

TG and DTA data were simultaneously recorded on a Rigaku Thermoflex TG8101D in vacuo ($\fallingdotseq 10^2$ Pa). About 10 mg of cesium formate was weighed into a platinum crucible; α-Alumina was used as a reference material.

The enthalpy changes for the phase transition and the melting were measured from DSC curves recorded on a Shinku-Riko DSC-1500 M5. About 10 mg of cesium formate was placed in an aluminum crucible, with α-alumina as a reference material. After the sample was in place, the sample chamber was purged with dry nitrogen gas, and the measurement was carried out in a closed system. The instrument was calibrated with the enthalpy changes for the phase transitions of potassium nitrate ($T_{tr} = 127.8$ °C, $\Delta H = 5.4$ kJ mol^{-1}) and potassium perchlorate ($T_{tr} = 299.6$ °C, $\Delta H = 13.8$ kJ mol^{-1}).[7]

Powder X-ray diffraction data were collected using Rigaku Geigerflex RAD-γA and RAD-3C diffractometers equipped with a high-temperature sample holder. The sample was ground and set on a platinum plate in a grove pack filled with dry nitrogen gas. The data were collected in the 2θ range 10−70° with a step-scan of 0.02° and fixed-time (20 s) counting procedure in vacuo ($\fallingdotseq 10^{-1}$ Pa). Cu Kα radiation was monochromatized at the counter side using a graphite monochromator.

Results and Discussions

The DTA curves are shown in Figure 1. Although no weight change was observed in the TG curve at the temperatures below the melting point, an endothermic peak was confirmed. The endothermic peak shows a shoulder on the higher temperature side. The powder X-ray diffraction patterns measured before and after the endothermic peak are shown in Figure 2.

The difference between the diffraction patterns obtained before and after the endothermic peak showed that the peak corresponded to a phase transition. When the sample was heated above the endothermic peak and cooled gradually, an exothermic peak was observed just below the temperature of the endothermic peak. This phenomenon corresponds to the thermal

* To whom correspondence should be addressed at the Department of Environmental Science.

⊗ Abstract published in *Advance ACS Abstracts,* May 1, 1995.

(1) Shishido, S.; Masuda, Y. *Nippon Kagaku Zasshi* **1971**, *92*, 309.
(2) Shishido, S.; Masuda, Y. *Nippon Kagaku Kaishi* **1973**, 185.
(3) Shishido, S.; Masuda, Y. *Nippon Kagaku Kaishi* **1976**, 66.
(4) Masuda, Y.; Hashimoto, K.; Ito, Y. *Thermochim. Acta* **1990**, *163*, 271.
(5) Braghetti, M.; Berchiesi, G. *Ann. Meeting, Chim. Inorg.* **1969**, 101. Ferloni, P.; Sanesi, M.; Franzosini, P. *Z. Naturforsch.* **1975**, *30a*, 1147.
(6) Izumi, F.; Asano, H.; Murata, H.; Watanabe, N. *J. Appl. Crystallogr.* **1987**, *20*, 411.
(7) *Kagaku Binran Kisohen (Handbook of Chemistry) II*, 3rd ed.; The Chemical Society of Japan; Maruzen: Tokyo, 1984; p 267.
(8) *International Tables for X-ray Crystallography*; International Union of Crystallography; D. Reidel Publishing Co.: Dordrecht, The Netherlands, 1985; Vol. III, p 259.

0020-1669/95/1334-3130$09.00/0

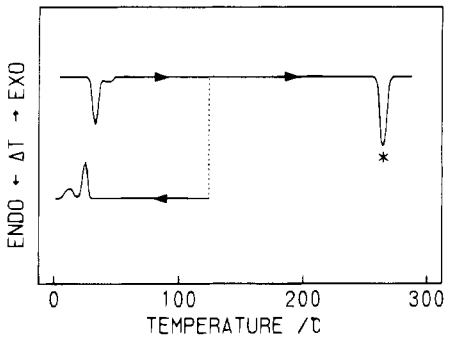

Figure 1. DTA curves of cesium formate. The asterisk indicates melting.

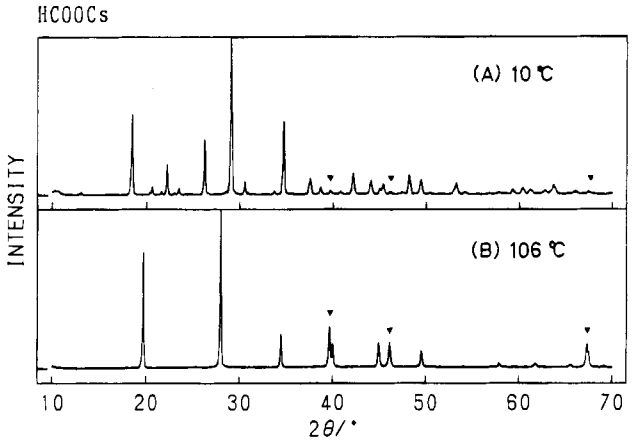

Figure 2. X-ray powder diffraction patterns measured before and after the endothermic event. ▼ indicates peaks corresponding to platinum used as a reference.

Table 1. Values of Enthalpy and Entropy Changes for the Phase Transitions of Cesium Formate

	T/°C	ΔH/kJ mol^{-1}	ΔS/J K^{-1} mol^{-1}
phase transition	36	6.87 ± 0.28	22.2 ± 0.9
	39[a]	4.52[a]	14.5[a]
melting	263	8.11 ± 0.33	15.1 ± 0.6
	266[a]	6.73[a]	12.6[a]

[a] Ferloni, P.; et al. *Z. Naturforsch.* **1975**, *30a*, 1447.

hysteresis effect, and the phase transition is classified as a reversible first-order transition. The exothermic peak had a discernible shoulder on the lower temperature side. However, no intermediate phase was detectable by careful diffraction analyses.

The values of the change in entropy and enthalpy for the phase transition and melting were obtained from the DSC measurement and are given in Table 1. They were reproducible but a little larger than those reported by Braghetti et al.[5] It is interesting that both the values of the enthalpy change (ΔH_{tr}) and entropy change (ΔS_{tr}) for the phase transition are comparable to those for melting (ΔH_{fus} and ΔS_{fus}, respectively). From this fact, a drastic structural change corresponding to the melting is expected to occur in the phase transition.

The X-ray diffraction lines of the phase before the transition could be indexed on the assumption that the crystal has an orthorhombic unit cell with the lattice parameters $a = 4.785(1)$, $b = 9.553(9)$, and $c = 15.927(2)$ Å. The diffraction pattern observed agrees with that calculated for the crystal structure, *Pbcm* (Table 2 and Figures 3 and 4).

All of the diffraction lines observed for the phase after the transition could be indexed on a cubic cell with a lattice constant of 4.500(5) Å. No extinction rules were found for both the general and special reflections. The z-value for the phase was

Table 2. Crystal Data for the Phase before the Phase Transition of Cesium Formate

Unit Cell Data	
space group	*Pbcm* (orthorhombic)
lattice consts	$a = 4.785(1)$ Å
	$b = 9.553(2)$ Å
	$c = 15.927(2)$ Å
Z	8

Atomic Fractional Coordinates (x, y, z) and Isotropic Thermal Parameters (B)

atom	x	y	z	B/Å^2
H[a]	0.8(1)	0.302(4)	0.128(3)	3.34
C	0.595(4)	0.302(4)	0.128(3)	5.81
O(1)	0.503(7)	0.408(2)	0.139(4)	3.03
O(2)	0.503(7)	0.196(2)	0.117(4)	3.03
$Cs^+(1)$	0.062(1)	0.25	0.25	2.51
$Cs^+(2)$	0.026(1)	0.25	0.00	2.51

Reliability Factors

R_I[b] = 5.29% R_F[c] = 3.49%

[a] The position of the H atom cannot be determined by means of X-ray diffraction, but the fractional coordinate obtained by the Rietveld analysis including the H atom is shown as a reference. [b] $R_I = \sum_k |I_k(o) - I_k(c)| / \sum_k I_k(o)$. [c] $R_F = \sum_k |[I_k(o)]^{1/2} - [I_k(c)]^{1/2}| / \sum_k [I_k(o)]^{1/2}$.

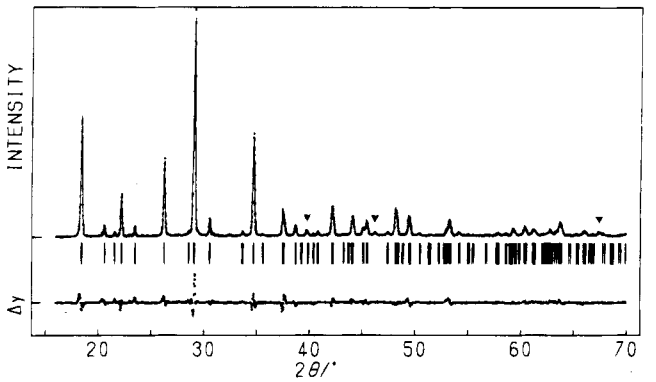

Figure 3. Observed (dotted), calculated (solid line), and difference (Δy, lower dotted line) X-ray powder diffraction profiles of the phase before the phase transition. Reflection positions are indicated by vertical bars. ▼ indicates peaks corresponding to platinum used as a reference.

anticipated to be unity from the density, roughly measured as 2.69 g cm^{-3}, where the z-value is the number of molecules in a unit cell. The diffraction pattern observed could be fitted satisfactorily with that calculated on the basis of *Pm3m* symmetry using the Rietveld method (Figure 5).[6] The structural parameters and the structure are also given in Table 3 and Figure 6, respectively.

In consideration of site symmetry for the space group, the positions at which the number of equivalent positions equals unity are *1a* (*m3m*) and *1b* (*m3m*), and their fractional coordinates are (0, 0, 0) and (0.5, 0.5, 0.5), respectively. This finding shows that the crystal has a high symmetry, and the orientation of the formate ion is thought to be disordered in this phase. In the Rietveld analysis, the structure of formate ion for the phase after the transition was assumed to be similar to that for the phase before the transition, and the formate ion was orientated as follows: the center of mass of the formate ion was situated in the *1b* (*m3m*) position, (0.5, 0.5, 0.5); Cs^+ was situated in the *1a* (*m3m*) position (0, 0, 0); the C and H atoms were situated in the *6f* (*4m.m*) positions; the O atoms were situated in the *24l* (*m..*) positions.

The structural change for the phase transition can be correlated to the changes of enthalpy and entropy. Figure 7 shows the three-dimensional frameworks connecting the eight cesium

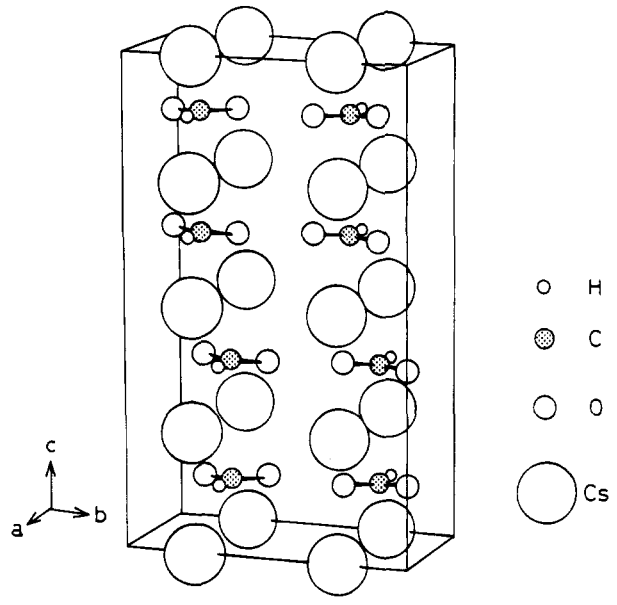

Figure 4. Crystal structure of the phase before the phase transition.

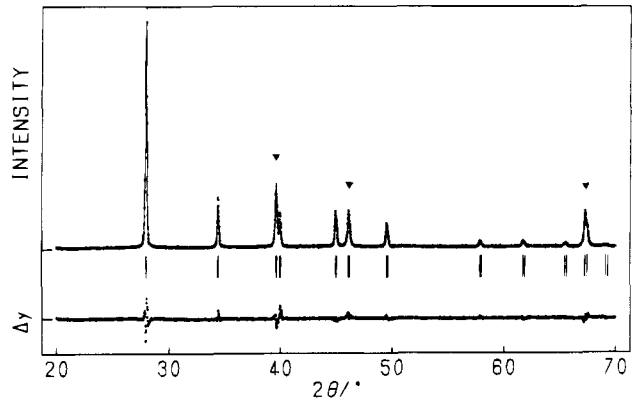

Figure 5. Observed (dotted), calculated (solid line), and difference (Δy, lower dotted line) X-ray powder diffraction profiles of the phase after the phase transition. Reflection positions are indicated by vertical bars. ▼ indicates peaks corresponding to platinum used as a reference.

Table 3. Crystal Data for the Phase after the Phase Transition of Cesium Formate

Unit Cell Data	
space group	*Pm3m* (cubic)
lattice consts	$a = 4.500(2)$ Å
Z	1

Atomic Fractional Coordinates (x, y, z) and Isotropic Thermal Parameters (B)

atom	x	y	z	B/Å^2
H[a]	0.8(1)	0.50	0.50	1.66
C	0.543(4)	0.50	0.50	3.60
O	0.50	0.554(1)	0.746(2)	1.37
Cs^+	0.00	0.00	0.00	7.32

Reliability Factors

R_I[b] = 2.16% R_F[c] = 1.37%

[a-c] See footnotes a-c, respectively, of Table 2.

atoms for the phases before and after transition. Little difference was noted between both the phases in the volumes of these frameworks. Therefore, the most remarkable change must be due to the orientation of the formate ion in the respective phases.

From the above viewpoint, the value of the entropy change for the phase transition can be explained on the basis of the change in the orientational freedom of the formate ion. Because the formate ion occupies a specific position in the structure

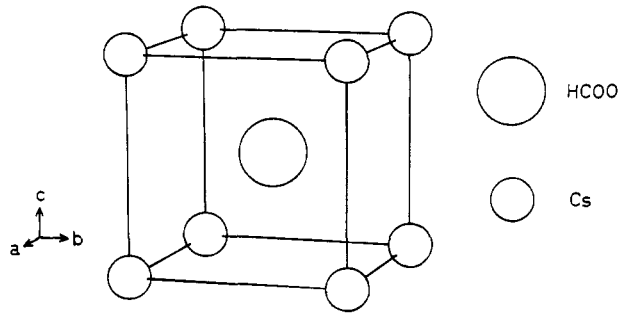

Figure 6. Crystal structure of the phase after the phase transition.

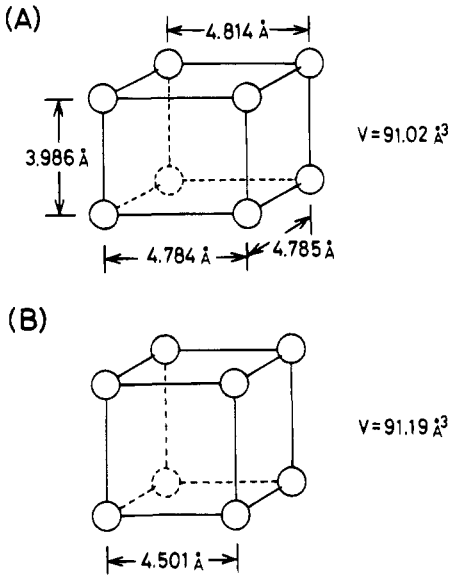

Figure 7. Three-dimensional frameworks connecting the eight cesium atoms of the phases before (A) and after (B) the phase transition.

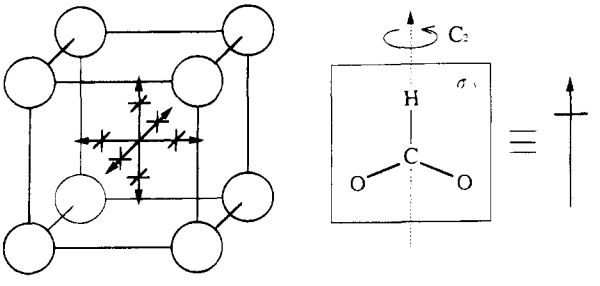

Figure 8. Schematic expression of the orientational freedom of formate ion for the phase after the phase transition.

before the transition, the orientational freedom is thought to be unity. On the other hand, the atomic configuration of formate ion is not determined in the phase after the transition. The orientational freedom, however, is estimated to be 12 as follow: it is possible for the formate ion to orient along the 6 directions ($\pm x$, $\pm y$, $\pm z$) in the cubic crystal system and each formate ion has a 2-fold rotational symmetry, thus the orientational freedom can be estimated at 12 (Figure 8).

The entropy change is calculated in accordance with the Boltzmann equation

$$\Delta S_{tr} = R \ln(n_{after}/n_{before})$$

where R is the gas constant and n_{after} and n_{before} represent the orientational freedom of the formate ion in the phase after and before the phase transition, respectively. Therefore

$$\Delta S_{tr} = R \ln(12/1) = 8.314 \times 2.485 \text{ J K}^{-1} \text{ mol}^{-1} = 20.7 \text{ J K}^{-1} \text{ mol}^{-1}$$

This value is in fair agreement with the observed one, 22.2 ± 0.9 J K^{-1} mol^{-1}. This fact shows that the transition seems to be classified as an order–disorder transition from the viewpoint of the orientation of formate ion.

Table 4 shows interatomic distances and angles for both of the phases. In the phase before transition, the cesium ion is surrounded by eight oxygen atoms of the formate ions and there are eight kinds of interatomic distances between cesium ion and oxygen (2.99(8)–3.67(7) Å). On the other hand, the cesium ion is surrounded by eight oxygen atoms in a regular cubic form in the phase after transition (3.22(1) Å). These atomic distances seem to be reasonable on the basis of the ionic radii of cesium ion.[8] The large value of enthalpy change for the transition may be due to the orientative change of the formate ion and the changes of these atomic distances in both of the phases.

Table 4. Interatomic Distances (Å) and Angle (deg)

	before transition of HCOOCs	after transition of HCOOCs
C–O	1.12(9)	
∠OCO	133.6	
M–O	2.99(8)	3.22(1) (×8)
	3.03(7)	
	3.13(8)	
	3.16(7)	
	3.44(8)	
	3.52(8)	
	3.54(7)	
	3.67(7)	

Acknowledgment. The authors gratefully acknowledge support from the Uchida Scientific Foundation. We are grateful to Professor Emeritus Y. Ito of Niigata University for discussions and encouragement. We also thank Professor P. Gallagher of The Ohio State University for his suggestions and valuable comments.

IC941183R